17th World Conference on Earthquake Engineering, 17WCEE
Sendai, Japan - September 13th to 18th 2020

Experimental investigation into the influence of slab restraint effect on flexural capacity of the reinforced concrete beam

Liping Wang [1], Shijian Yang [2], Licheng Jiang [3], Wenwen Luo [4], Wei Zhang [5]

[1] *Associate Professor, School of Civil Engineering and Architecture, Chongqing Univ. of Science and Technology, Chongqing 401331, China; wangliping98@163.com*
[2] *Graduate Student, School of Civil Engineering and Architecture, Chongqing Univ. of Science and Technology, Chongqing 401331, China.*
[3] *Graduate Student, School of Civil Engineering and Architecture, Chongqing Univ. of Science and Technology, Chongqing 401331, China.*
[4] *Lecturer, School of Civil Engineering and Architecture, Chongqing Univ. of Science and Technology, Chongqing 401331, China; luowenwen326@163.com.*
[5] *Graduate Student, School of Civil Engineering and Architecture, Chongqing Univ. of Science and Technology, Chongqing 401331, China.*

Abstract

The contribution of the slab to the flexural capacity of the beam in the RC (reinforced concrete) frame is one of the important factors achieving the "strong column weak beam" failure mechanism. The RC frame beams tend to elongate after flexural cracking and yielding. However, in RC frames, the restraint effect of the cast-in-place slab and the surrounding lateral resistant-system on the beam elongation resulted in a non-negligible compressive axial force of beams. Therefore, it affects the seismic performance of the beam and the failure mode of structures under strong earthquake. This study aims at obtaining the beam seismic performance with or without slab restraint effects. The test was conducted on a 1/2 scale interior beam-column-slab specimens including transverse beams. Under the cyclic loading, the elongations of beam were measured. The seismic performance and failure mode of the RC beam were compared by the beam-column specimens with or without slab. The results showed that the axial restraint effect of the cast-in-place slab was not significant on the beam elongation. A larger effective slab width to considering the contribution of slab was reasonable.

Keywords: reinforced concrete frame; axial restraint; beam elongation; cyclic loading; slabs

1. Introduction

During strong earthquakes, the behavior of beam-column-slab joint subassemblies are significant on the seismic performance of multistory RC frame buildings. Therefore, properly design of flexural behavior of beams is one of key factors to achieve strong column-weak beam mechanism when subjected to major earthquakes. However, the flexural strength of beams is affected by the beam elongation phenomenon [1, 2]. RC beam tend to elongate after beam flexural cracking and yielding, which primarily occurred at plastic hinge regions of beams [1]. And a beam could elongate freely in cyclic loading tests without any restraint conditions [3]. However, beam elongation in RC frames is restrained by surrounding structural components, such as columns. In turn, compressive axial force develops in the beam, thereby enhancing the flexural strength [4, 5]. And the restraint could be partially enforced by cast-in-place RC slabs through continuity and high in-plane stiffness [6]. For simplicity, the participation of slabs in resisting lateral loads was normally considered by assigning an effective slab flange width [7, 8], which accounts not only for the negative bending resistance provided by slab reinforcements, but also for the effects of restraining beam elongations. This paper present a series of experiments to further examine the influence of cast-in-place RC slabs on beam elongations and flexural strength of beams.

2. Construction of Specimens

2.1 Test setup and specimen properties

A 1/2-scale beam-column-slab subassembly including transverse beams was tested. The specimen represented the interior beam-column-slab subassemblies of a multibay, multistory RC frame prototype building with an 8-m span length and a 3.2-m story height. The presence or not of the slab was considered as test variable. For purposes of comparison, the Specimen 3N, an interior beam-column subassembly without the slab and transverse beam, was chosen from previous experiments [2]. Considering the complex factors on the effective width of slab [5, 9-16], a sufficient slab width should be required for specimen design. Therefore, the slab width of Specimen 3SA was 3600 mm for this test. The specimens were designed and detailed based on the seismic design provisions in ACI 318 [17] and the Chinese seismic design code [18]. The dimension and reinforcing details of Specimen 3SA were shown in Fig. 1. The effective beam length and column height were 4 m, 1.6 m respectively. The beam had a width of 250 mm and height of 400 mm. The column cross-sectional dimension was 350 mm in the loading direction and 300 mm in the transverse direction. The slab cross-sectional dimensions was 4260 mm in the loading direction and 3600 mm in the transverse direction, and the thickness of slab was 80 mm.

Because the experiments focused on the flexural behavior of beams, the column was heavily reinforced, so were the transverse reinforcement of the beam and column. The longitudinal reinforcement had a 16-mm (D16) diameter for the beams and 25-mm (D25) diameter for the columns. Rectangular hoops made of D10 bars were used as beam transverse reinforcement and were uniformly distributed at a center-to-center spacing of 90 mm. The transverse reinforcement of the columns contained two overlapping D12 hoops with a spacing of 80 mm. The beam-column joint contained two overlapping D12 hoops with a spacing of 75 mm. There were two reinforcement layers in the slab. For each layer, the slab was reinforced by D6.5 bars with a spacing of 160 mm in the loading and transverse direction.

The dimension and reinforcing details of Specimen 3N was identical to that of Specimen 3SA. Details could be obtained from reference [2]. The reinforcing details of transverse beam of Specimen 3SA was the same as that of the beam along the loading direction. The clear thickness of concrete cover was specified as 15 mm for the beams, 20 mm for the columns and 15mm for the slab. Table 1 gives the yield strengths of the reinforcing bars and cylinder compressive strength of concrete after the completion of the test.

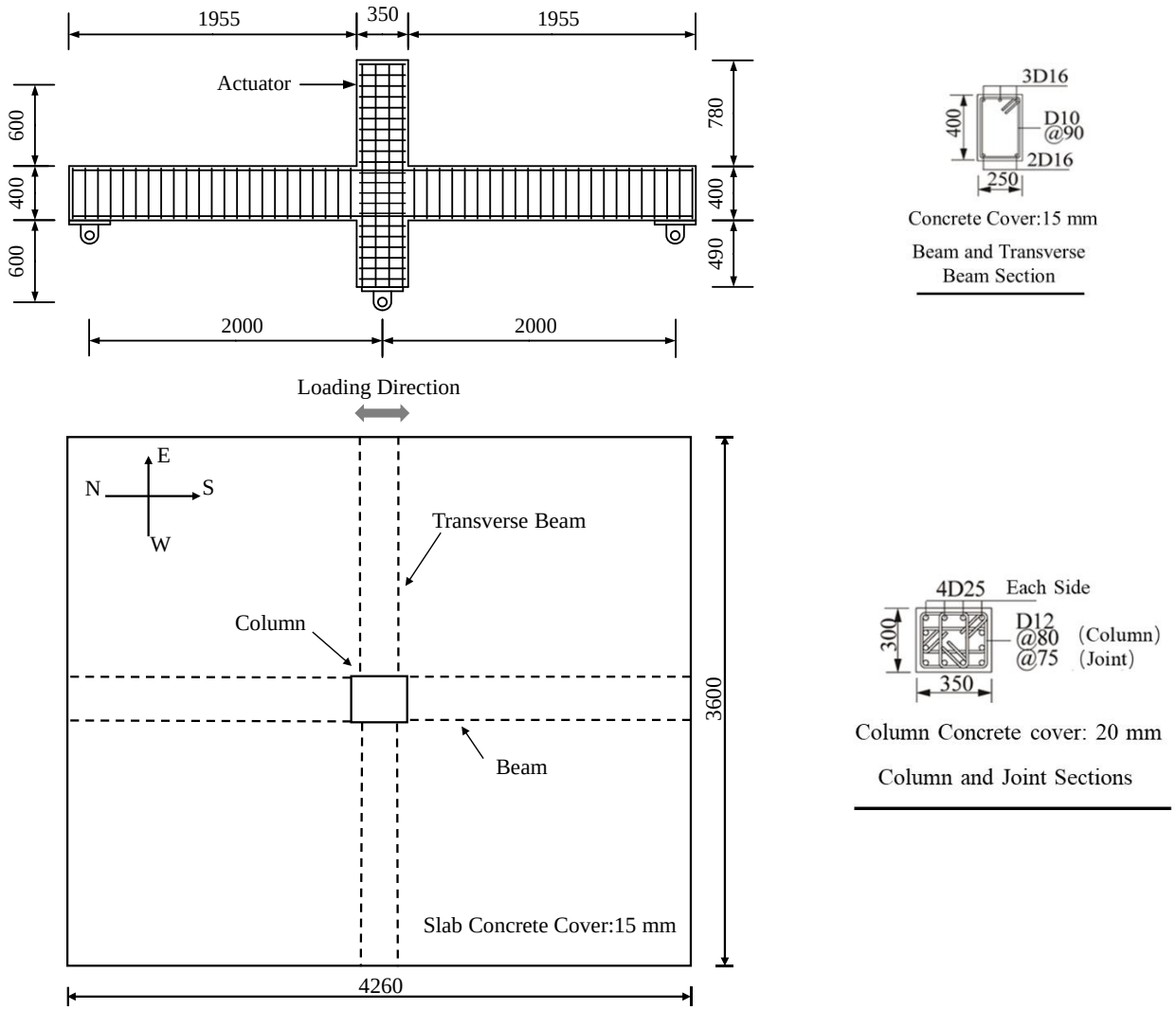

Fig.1 - Dimensions (in millimeters) and reinforcing details of Specimen 3SA.

Table 1 Test specimens and material properties

Specimen	Yield strength of reinforcing bars (MPa)					Cylinder concrete strength (MPa)
	D6.5	D10	D12	D16	D25	
3SA	428	678	622	471	491	38.4
3N	-	595	545	493	473	28.7

2.2 Loading protocol and instrumentation

Fig.2 shows the test setup. The test was carried out by displacement quasi-static cyclic loading by a 500-kN loading capacity hydraulic actuator which was connected with column top by pin connection. To prevent out plane movement of the specimen during cyclic loading, four steel bracing frames were mounted around the specimens and fully anchored to the reaction floor.

Fig. 3 shows the lateral loading history. Each specimen had eight drift levels including 0.375%, 0.5%, 0.75%, 1%, 1.5%, 2%, 3% and 4%.The drift was defined as the lateral displacement of the specimen divided by the effective height of the column. LVDTs were used to measure the horizontal displacements at column top, beam ends. Based on the measured beam horizontal movements at various locations, the overall beam elongation was determined. Two tension or compression load sensors were embedded in the vertical struts to measure the vertical reaction force at beam ends that could gain the bending moment of beams.

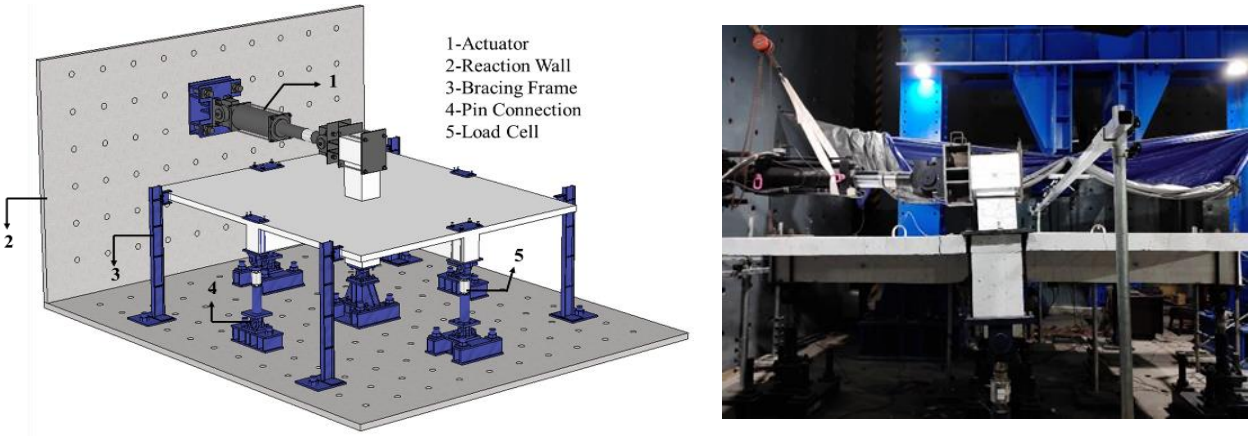

(a) Schematic Drawing （b）Photograph

Fig.2 - Test Setup.

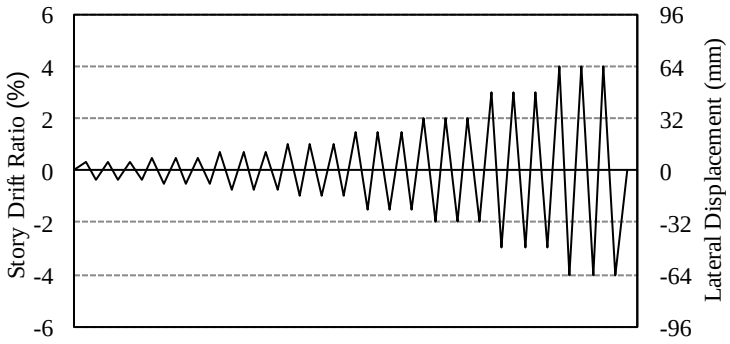

Fig.3 - Lateral load history.

3. Experiment Results

3.1 Hysteretic response

Fig. 4 shows the hysteretic curves of lateral load versus drift for the Specimen 3SA and 3N. The measured strains indicated that the flexural yielding occurred at about 0.95% and 1.12% drift in the beam top reinforcement of Specimen 3SA and 3N, respectively. And the flexural yielding drift was about 0.70% and 0.92% drift in the beam bottom reinforcement, respectively. Specimens 3N as well as 3SA presented a yield plateau in the response envelopes. And the strength degradation phenomenon did not present during the whole loading process. However, Specimens 3SA and 3N had an obvious pinching effect indicated the longitudinal reinforcement developed a large bond slip in plastic hinge regions of beam and joint regions. The bond slip effect was evidenced by the damage patterns of the specimen. The hysteretic loops of Specimen 3SA was much fuller than in Specimen 3N, due to the participation of slab. At 2% drift, the lateral load of the Specimen 3SA and 3N was about 233kN and 117kN, respectively. The lateral load of Specimen 3SA was about 2.0 times that of Specimen 3N. The flexural capacity and stiffness of beams was enhanced by the participation of slab.

The participation of slab in resisting lateral loads was usually considered by assigning an effective slab flange width. So the slab and beam could be treat as a T-shape beam. According to the suggestions of reference [17], the effective flange width of the slab was taken as the web width plus 16 times slab thickness, herein it is 1530 mm. Then the flexural capacity $M_{u,0}$ could be obtained through section analysis without considering the strain hardening effects of reinforcement. The lateral loading capacity $F_{u,0}$ predicted based on $M_{u,0}$, specimen dimension, and supporting condition is shown by horizontal dashed lines in Fig.4. For Specimen 3N, the predicted lateral loading capacity $F_{u,0}$ can also be obtain in the same way, without considering the participation of slab. The predicted lateral loading capacity of Specimen 3N was at considerable agreement with test data. But, for Specimen 3SA, the lateral loading capacity was 1.45 times that of the predicted value at 2% drift. It seems that a larger effective flange width should be supposed.

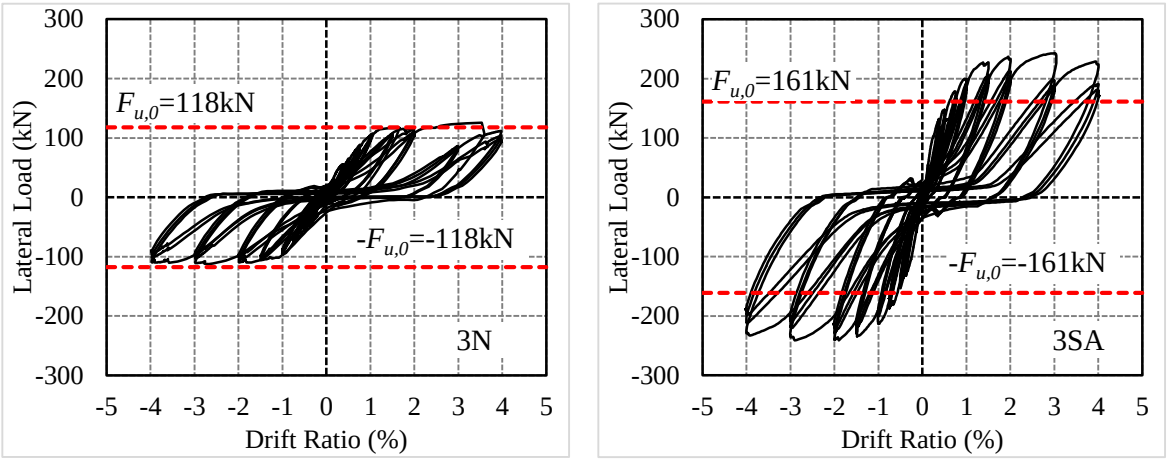

Fig.4 - Hysteretic response of lateral load versus drift.

3.2 Damage patterns of beams

The damage patterns in plastic hinge regions of beams for Specimen 3SA, 3N at 2% drift and 4% drift were shown in Figs.5 and 6. The performance of the specimens (3SA and 3N) was dominated by flexure, and the lateral drift beyond beam yielding was accommodated mainly by bond slip in the beam plastic hinge regions and the joint. Beam flexural cracks occurred at first positive drift level of 0.375% for both Specimen 3SA and 3N. The flexural cracks at the beam column interface became much wider than 2mm, by 1.5% drift and 2% drift for Specimen 3SA and 3N, respectively. The cracks penetrated the entire beam depth, and could not be completely closed in the subsequent loading reversals. Very few new cracks were further developed in the joints of Specimens 3SA and 3N beyond 2% drift. Damage to the beams due to spalling of concrete cover occurred at 3% drift in Specimen 3SA and 3N, but was limited within small regions.

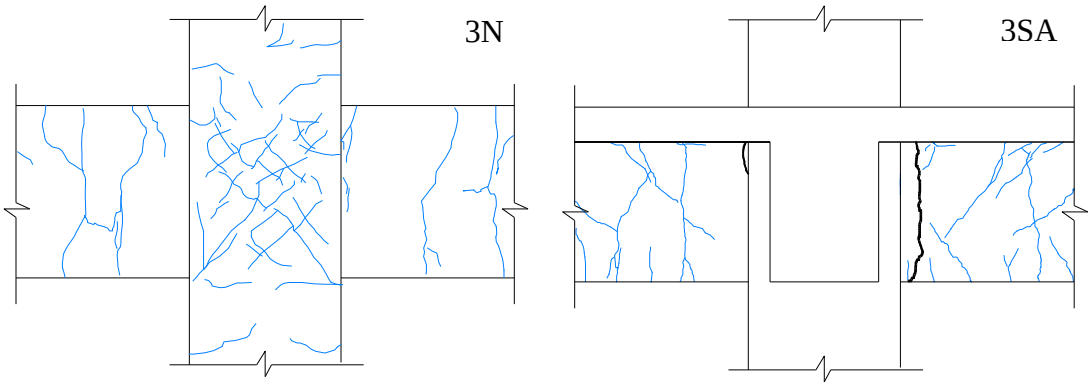

Fig.5 - Damage condition of specimens at 2% lateral drift.

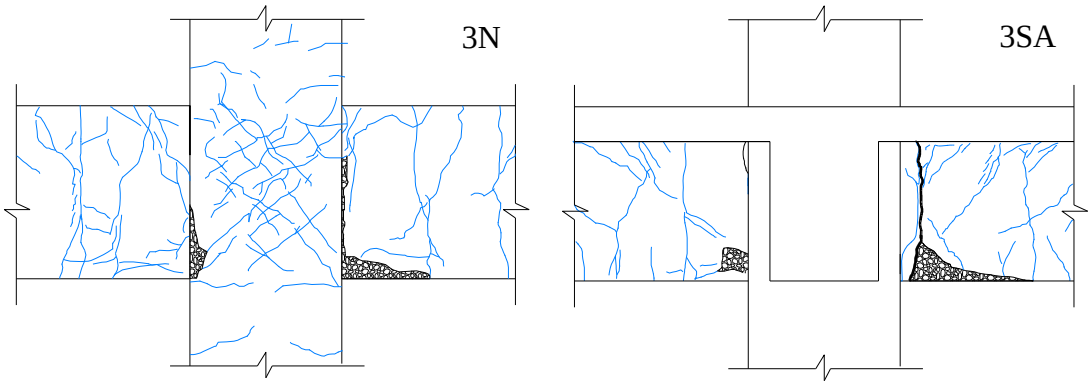

Fig.6 - Damage condition of specimens at 4% lateral drift.

Fig.7 shows the damage patterns in the slab for Specimen 3SA at 2% drift by top view. The cracks on the top of slab occurred at first positive drift level of 0.375%, which passed through the entire width of slab in the transverse direction. Inclined cracks on the top of slab was first found at the 0.5% drift, and the maximum width of which was approximately 0.3mm. The angle between the inclined cracks and the direction of the beam was about 45 degrees. Many new cracks on the top of slab were further developed with the lateral cyclic loading until 2% drift.

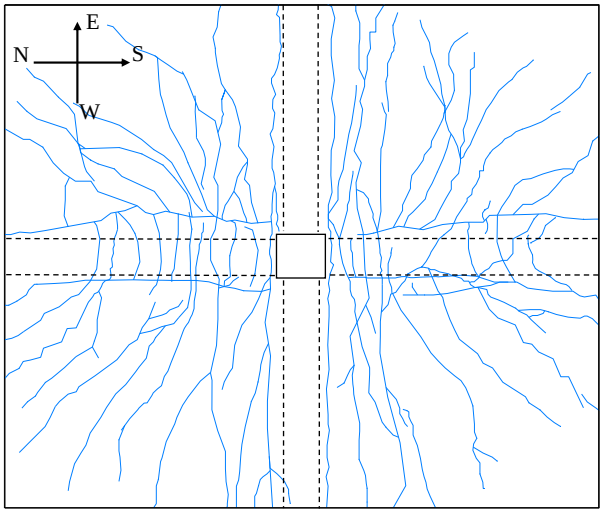

Fig.7 Cracking patterns on the top of slab for Specimen 3SA at 2% drift.

3.3 Beam elongation

The total beam elongation of the specimens (3SA and 3N) was contributed from the two beams of a specimen one subjected to negative bending and the other subjected to positive bending [2], was determined based on the measured horizontal displacement at beam ends. Fig. 8 shows the beam elongation history of Specimen 3SA and 3N. The geometric elongation accounted a great portion of total beam elongation under lower drift ratios. But, with increased level of cyclic lateral drifts, residual crack opening gradually accumulated and started to account for a greater portion of beam elongation. At 2% drift, the maximum beam elongations of Specimen 3SA was 6.54 mm equivalent to about 1.6% of the beam depth. And the residual elongation was about 4.30 mm about 1.1% of the total elongation. At 4% drift, the elongation was as high as 14.22mm, about 3.56% of the beam depth. The residual elongation was about 11.88mm about 83.5% of the total elongation. Compared with Specimen 3N, the maximum beam elongation of Specimen 3SA was about 0.8 times that of Specimen 3N at 2% and 4% drift.

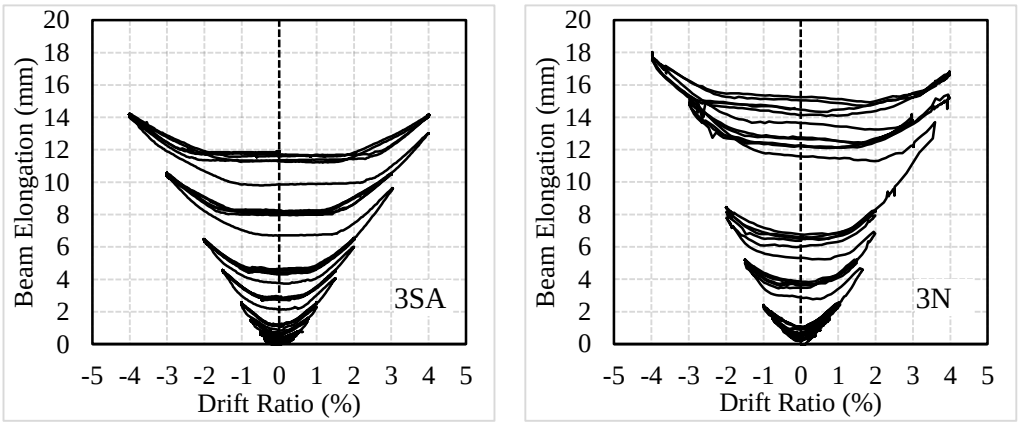

Fig.8 - Beam elongation history.

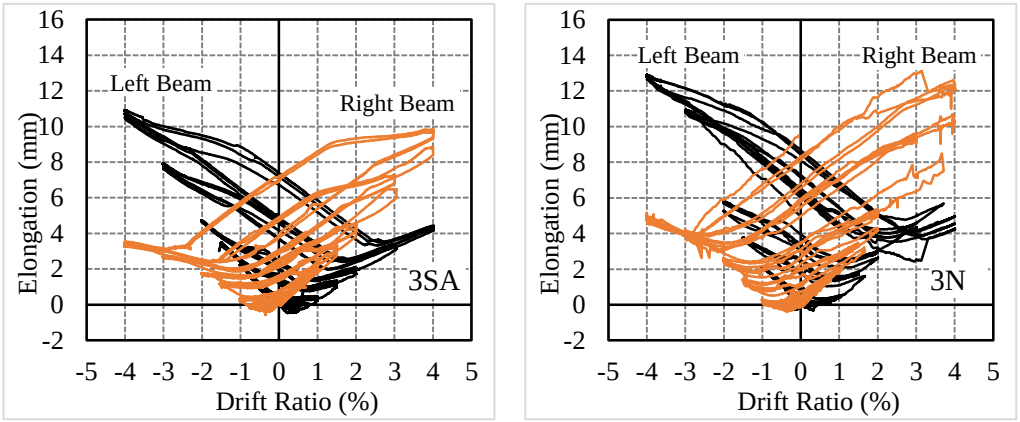

Fig.9 - Elongation of single beam versus lateral drift.

Fig.9 shows the one-side beam elongation of Specimen 3SA and 3N. The one-side beam elongation was determined based on the measured horizontal displacement at beam ends and the calculated horizontal displacement of joints. The horizontal displacements of joint were derived from geometric relationship between column top and joint, according to the horizontal displacement of column top. The flexural deformation of columns was ignored because the column behaved in elastic manner during the whole loading process. Beyond 1.5% drift, positive bending resulted in greater beam elongation than negative bending for Specimen 3SA and 3N. The positive bending induced one-side beam elongation of Specimen 3SA was relatively smaller than that of Specimen 3N, as well as the negative bending induced one-side beam elongation.

The horizontal displacements of the slab ends was not measured for Specimen 3SA. But the residual elongation of slab was obtained by directly measuring the length of the slab after the completion of the test. The residual elongation was about 10mm. And this magnitude of residual elongation means that the slab also experienced great elongation during lateral cyclic loading. Under the considered boundary condition of the Specimen 3SA, it seemed that the effect of slab on beam elongation was not significant.

3.4 Effects of slab on beam flexural strength

Fig.10 shows the envelope curves of beam moment versus drift ratios for Specimen 3SA and 3N. The beam moment was determined based on the tension and compression load cells embedded in the vertical struts at beam end. Compared with Specimen 3N, the positive and negative bending moment were enhanced by the participation of slab. At 2%, the positive and negative bending moment of Specimen 3SA was about 1.66 and 1.94 times that of Specimen 3N, respectively.

The predicted flexural strength $M_{u,0}$ for Specimen 3N is shown by the horizontal red dashed lines in Fig.10(a) and Fig.10(b). And the predicted flexural strength $M_{u,0}$ for Specimen 3SA under negative bending is shown by the horizontal blue dashed lines in Fig.10(b). The actual flexural strength of Specimen 3SA under negative bending was underestimated. It seems that a larger effective slab width is reasonable for considering the contribution of slab on the bending moments of beam.

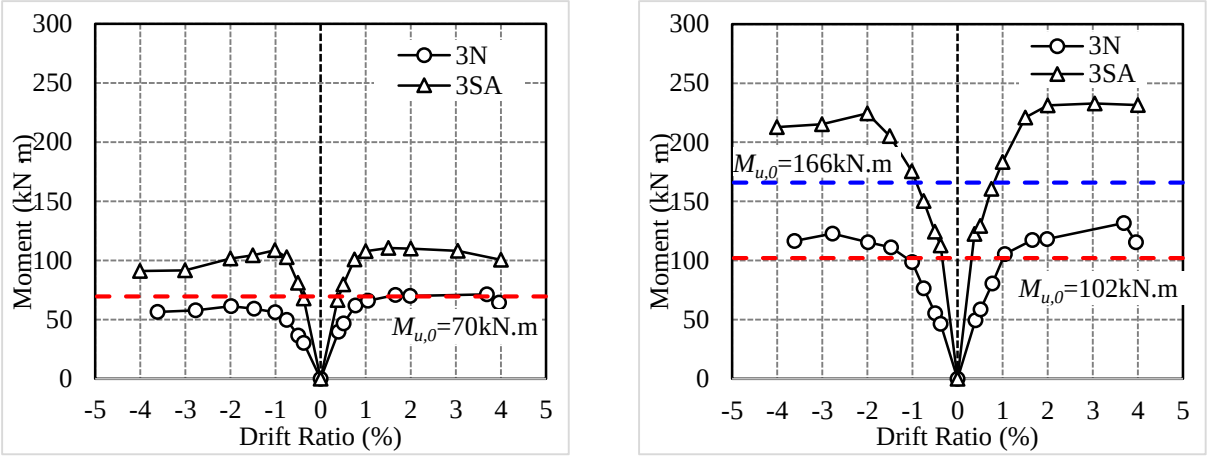

(a) positive moment (b) negative moment

Fig 10. Moments in beams versus drift ratio: (a) positive moment for resisted by two bottom bars with or without slab; (b) negative moment for beams resisted by three top bars with or without slab.

4. Conclusions

Experiments were conducted to examine the effects of cast-in-place RC slabs on the beam elongations and flexural strength of beams. The following observations and preliminary conclusions were made from the tests:

(1) The flexural capacity of beams was enhanced by the participation of slabs.

(2) Under the considered boundary condition of this test, there was little difference in the elongation of beams, whether with the participation of slab or not. It seemed that the effect of slab on beam elongation was not significant.

5. Acknowledgements

The authors are grateful for the financial supports received from the National Natural Science Foundation of China (No. 51808087) and Chongqing Science and Technology Commission (cstc2018jcyjAX0695 and cstc2018jcyjAX0052). The authors also gratefully acknowledge Prof. Tian Ying from Univ. of Nevada for his valuable advice to experimental design and result analysis.

6. Copyrights

7. References

[1] Fenwick R and Fong A (1979): The Behaviour of Reinforced Concrete Beams Under Cyclic Loading. University of Auckland, New Zealand, *Research Report* no. 176.

[2] Wang L, Tian Y, Luo W, et al (2019): Seismic Performance of Axially Restrained Reinforced Concrete Frame Beams[J]. *Journal of Structural Engineering*, 145(5): 04019019.

[3] Ashtiani, M. S., R. P. Dhakal, and A. N. Scott (2014): Seismic performance of high-strength self-compacting concrete in reinforced concrete beam column joints. *J. Struct. Eng.* 140 (5): 04014002.

[4] Zerbe HE, Durrani AJ (1989): Seismic response of connections in two-bay R/C frame subassemblies. *ASCE Journal of Structural Engineering* 115(11): 2829–2844.

[5] Zerbe, H. E., and A. J. Durrani (1990): Seismic response of connections in two-bay reinforced concrete frame subassemblies with a floor slab. *ACI Struct. J.* 87 (4): 406–415.

[6] Qi, X., Pantazopoulou, S. J. (1991): Response of RC frame under lateral loads. *Journal of Structural Engineering*, 117(4), 1167-1188.

[7] French, C. W., Boroojerdi, A. (1989): Contribution of R/C floor slabs in resisting lateral loads. *Journal of Structural Engineering*, 115(1), 1-18.

[8] French, C. W., Moehle, J. P. (1991): Effect of Foor Slab on Behavior of Slab-Beam-Column Connections. *Special Publication*, 123, 225-258.

[9] Durrani A J, Zerbe H E (1987): Seismic resistance of R/C exterior connections with floor slab[J]. *Journal of Structural Engineering*, 113(8): 1850-1864.

[10] LaFave J M, Wight J K (1999): Reinforced concrete exterior wide beam-column-slab connections subjected to lateral earthquake loading[J]. *Structural Journal*, 96(4): 577-585.

[11] Shin M, LaFave J M (2004): Reinforced concrete edge beam-column-slab connections subjected to earthquake loading[J]. *Magazine of Concrete Research*, 56(5): 273-291.

[12] Gunasekaran U, Ahmed S M (2014): Experimental investigation into the seismic performance of slabs in RC frame joints[J]. *Magazine of Concrete Research*, 66(15): 770-788.

[13] Cheung P, Paulay T and Park R (1987): A Reinforced Concrete Beam Column Joint of a Prototype One-Way Frame with Floor Slab Designed for Earthquake Resistance. University of Canterbury, New Zealand, *Research Report* 87-6.

[14] Ye L, Qu Z, Ma Q et al (2008): Study on ensuring the strong column-weak beam mechanism for RC frames based on the damage analysis in the Wenchuan earthquake. *Building Structure*, 38(11): 52-59.

[15] Paulay, T. and Park, R. (1984): Joints in Reinforced Concrete Frames Designed for Earthquake Resistance," *Research Report* No.84-9, Department of Civil Engineering, University of Canterbury, Christchurch, 71 pp.

[16] Pantazopoulou, S. J.; Moehle, J. P.; and Shahrooz, B. M. (1988),"Simple Analytical Model forT-Beams in Flexure," *Journal of Structural Engineering*, ASCE, V. 114, No. 7, pp. 1507-1523.

[17] ACI (American Concrete Institute) (2014): Building code requirements for structural concrete. ACI 318. Detroit: ACI.

[18] CMC (China Ministry of Construction) (2010): Code for seismic design of buildings. GB 50011. Beijing: CMC.

